RESEARCH ARTICLE

LUMINESCENCE WILEY
The Journal of Biological and Chemical Luminescence

Sulfur quantum dots as a novel platform to design a sensitive chemiluminescence probe and its application for Pb^{2+} detection

Sima Mojarrad[1] | Abdolhossein Naseri[1] | Tooba Hallaj[2]

[1]Department of Analytical Chemistry, Faculty of Chemistry, University of Tabriz, Tabriz, Iran

[2]Cellular and Molecular Research Center, Cellular and Molecular Medicine Institute, Urmia University of Medical Sciences, Urmia, Iran

Correspondence

Abdolhossein Naseri, Department of Analytical Chemistry, Faculty of Chemistry, University of Tabriz, Tabriz 5166616471, Iran.
Email: a_naseri@tabrizu.ac.ir

Tooba Hallaj, Cellular and Molecular Research Center, Cellular and Molecular Medicine Institute, Urmia University of Medical Sciences, Urmia 5714783734, Iran.
Email: hallaj.t@umsu.ac.ir

Abstract

The monitoring of Pb as a hazardous heavy metal element for the environment and human health is of high importance. In this study, a simple and sensitive chemiluminescence (CL) probe based on sulfur quantum dots (SQDs) was designed for the determination of Pb^{2+}. To the best of our knowledge, this is the first report on the analytical application of the CL method based on SQDs. For this purpose, SQDs were synthesized using a simple hydrothermal method and characterized using transmission electron microscopy, Fourier transform infrared spectroscopy, X-ray photoelectron spectroscopy and X-ray diffraction. Then, the direct CL of SQDs elicited by common oxidants was investigated. The highest CL intensity was observed for the SQDs–KMnO$_4$ reaction, and its CL mechanism was studied. We indicated that the CL intensity of introduced system can be diminished as a result of the interaction between Pb^{2+} and SQDs, and exploited this fact for designing a CL-based probe for the determination of Pb^{2+}. The CL intensity of the SQDs–KMnO$_4$ reaction was linearly quenched using Pb^{2+} in the range 50–2000 nM with a limit of detection of 16 nM (S/N = 3). The probe was used for the determination of Pb^{2+} in different water samples and the recovery results (95.2–102.8%) indicated the good analytical performance of the developed method.

KEYWORDS

chemiluminescence, heavy metals, sulfur quantum dots

1 | INTRODUCTION

Colloidal luminescent semiconductor quantum dots (QDs) such as CdS, CdSe, CdSe/ZnS, PbS InPb/ZnS, and so on have found useful application in many areas of science due to their exceptional photophysical characteristics.[1,2] However, the presence of hazardous heavy metals (including Cd and Pb) and the complicated preparation methods of the prevalent QDs, can limit their application. Therefore, the substitution of these QDs with pure elemental QDs such as carbon,[3,4] phosphorous,[5,6] and silicon[7,8] QDs is highly desirable.

The new member of pure elemental QDs is sulfur QDs (SQDs), which was reported for the first time by Li and coworkers in 2014.[9]

After that, these green QDs have attracted exceptional attention in different fields including sensing[10–12] bioimaging,[13] light-emitting devices,[14] and photocatalysis[9] due to their unique properties such as excellent water dispersibility, stable photoluminescence, and non-toxicity as well as intrinsic antibacterial activity. In addition, the presence of sulfate and sulfite functional groups on the surface of SQDs provides tunable optical properties in addition to the ease of functionalization.[15]

Even though SQDs have been applied for the detection of some biological and environmental compounds using electrochemical,[16] colorimetric,[13,17] and fluorometric[18–22] methods, there has been no report about analytical applications of SQD-based chemiluminescence

(CL) reactions. Among various analytical methodologies, CL detection with high sensitivity towards a wide range of species, short analysis time, eliminated background, and light scattering effects, wide calibration range, low limits of detection, and simple instrumentation has been accepted as a desired analytical tool for the trace determination of organic and inorganic analytes including ions.[23–26] However, the low quantum yield of traditional CL reactions can restrict their analytical applications. In this sense, many efforts have been targeted to enhance the CL intensity of weak reactions and improve their analytical applications. For example, various nanomaterial and QD-based CL systems have been introduced and their analytical applications were investigated. QDs can act as catalysts, emitters, and/or contributors in the energy transferring process during the CL reaction.[27–29] Although the CL behaviour of SQDs has been slightly studied, no analytical method based on SQD CL has been reported.[30] Several nanomaterial-based CL systems have been reported for environmental and biological analysis of different ions including Pb.[24,25,31]

Pb, which is widely used in various industries and compounds (such as fertilizers, plastic stabilizers, and so on), has been known as a heavy metal element hazardous for the environment and human health. The accumulation of Pb ions in the human body can affect blood production and circulation system and cause headaches, dizziness, fatigue, memory loss, irritability, and mental retardation.[32] Therefore, the development of fast, sensitive, and accurate procedures for the determination of Pb is of high importance from the environmental and analytical points of view. A wide variety of analytical methodologies for the determination of Pb has been reported in the literature including colorimetry,[17,33] fluorescence,[34,35] and CL methods.[36–39]

In this study, a SQD-based CL method was developed for the detection of Pb ions. First, the direct CL of the hydrothermally synthesized SQDs was investigated and SQDs–KMnO$_4$ was introduced as a CL system. Then, it was used for the sensitive determination of Pb ions in real water samples with satisfactory results. Our literature review shows that this is the first report on the analytical application of the CL method based on SQDs.

2 | EXPERIMENTAL

2.1 | Apparatus

Chemiluminescence signals were measured using a Junior LB 9509 luminometer (Berthold Technologies, Germany) with a batch injection system. The fluorescence spectra were recorded using an F-2500 spectrofluorimeter (Hitachi, Japan). UV–vis spectra were recorded using a PG-instruments (T80+, China) with a 1-cm quartz cell. The size and morphology of SQDs were characterized using a transmission electron microscope (TEM) LEO 906 (Zeiss, Germany) with an accelerating voltage of 100 kV. A Fourier transform infrared (FT-IR) spectrophotometer, Tensor 27 Bruker, was used to record the IR spectra. A Siemens D500 X-ray diffractometer (Germany) with a monochromated Cu K$_\alpha$ radiation source ($\lambda = 1.54$ Å) was used to measure the X-ray diffraction (XRD)

patterns. An X-ray photoelectron spectroscopy (XPS) system, FlexPS (Specs, Germany), was applied for XPS analysis.

2.2 | Reagents and materials

All chemicals were of analytical grade and used without further purifications. Double-distilled water (ORUM SOO, Urmia, Iran) was used throughout the experiments. Sulfur powder, Pb(NO$_3$)$_2$, NaOH and KMnO$_4$ were purchased from Merck (Darmstadt, Germany). Polyethylene glycol (PEG-400) was purchased from Sachmon (Korea). Stock solutions [Pb(NO$_3$)$_2$ (10^{-2} M), NaOH (3 M) and KMnO$_4$ (10^{-3} M)] were diluted daily to prepare the working solutions.

2.3 | Synthesis of SQDs

SQDs were synthesized by means of a hydrothermal reaction.[40] In a typical procedure, 500 µl of PEG-400 was added to 10 ml of NaOH (2 M) with stirring, then 0.3 g of sulfur powder was added to the obtained solution. After 10 min stirring, the mixture was transferred to a Teflon-lined autoclave chamber, sealed, and placed into the oven at 170°C for 4 h and then naturally cooled down to ambient temperature. The resulting yellow solution containing SQDs was centrifuged at 6000 rpm for 10 min to remove large particles. Then, the supernatant was diluted 10-fold and stored in the refrigerator (4°C) for subsequent experiments. The concentration of the SQDs solution was calculated according to the concentration of the sulfur source.

2.4 | General procedure for CL monitoring

The CL measurements were performed in the batch condition with a final volume of 1 ml. For this purpose, 200 µl of the prepared SQDs (3 g L^{-1}) and 100 µl of NaOH (0.1 M) solutions were added into the CL cell. Then, a suitable volume of Pb (10^{-5} M) was pipetted into the cell [to make a series of concentrations of Pb^{2+} (0.05–2 µM)] and diluted to 950 µl with double-distilled water. After injection of 50 µl KMnO$_4$ solution (10^{-3} M), the CL signal was monitored versus time for 50 s. The peak integration was used as an analytical signal.

2.5 | Preparation of real water samples

For real sample analysis, tap water samples were taken from our laboratory in Urmia (Iran) and the spring and well water samples were collected from surrounding areas of Urmia (Iran). The spiked samples with three different concentrations (0.2, 0.5, and 2.0 µM) were prepared by adding known amounts of Pb (10^{-4} M) into 10 ml of the original water samples. No pretreatments were need before the analysis of water samples. An appropriate amount of all water samples was added into the CL cell and measured according to the general procedure.

3 | RESULTS AND DISCUSSION

3.1 | Characterization of SQDs

We used a simple hydrothermal method for the synthesis of SQDs using sulfur powder as a sulfur source and PEG-400 as a surface modification agent. The TEM images (Figure 1a) of the synthesized SQDs indicated that they are monodisperse and spherical shape nanoparticles with a size distribution in the range 50 ± 30 nm.

The FT-IR spectrum of SQDs was recorded to determine their surface functional groups. As shown in Figure 1b, the characteristic peaks of PEG 400 appeared in the SQD spectrum at 999 (C–O–C), 1115 and 1250 (C–O–H), 1643 (C=O), 2887 (C–H) and 3444 (–OH) cm^{-1}. Furthermore, the peaks at 521 and 665 cm^{-1} can be assigned to the S–S and S–O bands respectively.[41] The observed similarity between the FT-IR spectra of PEG 400 (Figure S1) and SQDs indicated that PEG 400 acts as a capping agent on the surface of SQDs and there was no chemical interaction between PEG 400 and SQDs.[17]
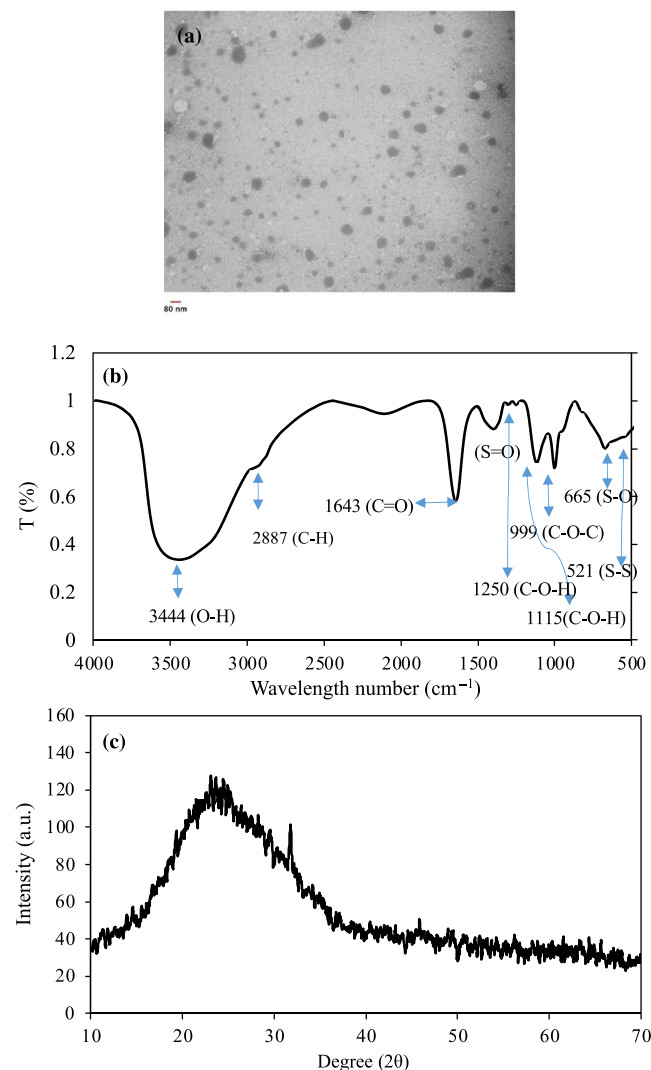
The XPS spectrum of as-prepared SQDs (Figure S2) confirmed the existence of C, O, and elements in the structure of SQDs. The high-resolution spectrum of S 2p of SQDs consisted of several peaks. Five peaks recognized in the high-resolution XPS spectrum of S, located at 160.3, 161.0, 162.1, 163.5, and 164.4 eV, were attributed to the elemental sulfur. Additionally, similar to the previous works, in which the oxidized sulfur composition of SQDs appeared in the binding energy > 166 eV, the peaks located at binding energies of 166.8, 167.6, and 169.1 eV could be assigned to SO_2^- ($2p^{2/3}$), SO_2^{2-} ($2p^{1/2}$), and/or SO_3^{2-} ($2p^{2/3}$), and SO_3^{2-} ($2p^{1/2}$), respectively.

The XRD pattern of the SQDs (Figure 1c) in which a peak appeared at $\sim 2\theta = 22°$ confirmed the amorphous structure of the SQDs.[30]

Moreover, the optical properties of SQDs were studied by recording their ultraviolet–visible (UV–vis) light absorption and fluorescence spectra. Three peaks appeared at $\sim$250, 300 and 366 nm of the UV–vis absorption spectrum of the SQDs (Figure 2a). These could be ascribed to the n→σ* electron transition related to nonbinding electrons of S_2^{2-} and S_8^{2-} adsorbed on the surface of the SQDs. The prepared SQDs indicated that the excitation depended on

FIGURE 1   (a) TEM image of the prepared SQDs, (b) FT-IR spectrum of the SQDs, and (c) XRD pattern of the SQDs
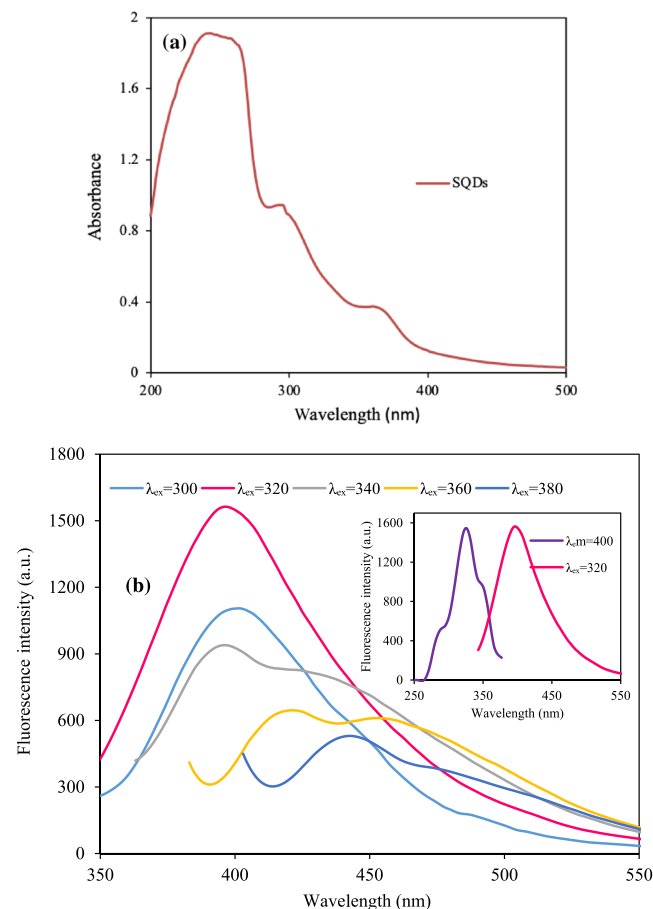

FIGURE 2   (a) Absorption spectrum of the SQDs sample, (b) fluorescence spectra of the SQDs excited at different wavelengths

fluorescence behaviour. As shown in Figure 2b, with varying the excitation wavelength from 320 to 420 nm, the fluorescence spectra of the SQDs shifted to higher wavelengths. This can be attributed to the various sizes and surface states of the SQDs.[17,19] The maximum emission intensity was obtained at the 320 nm excitation wavelength that was placed at 400 nm.

3.2 | Direct chemiluminescence of SQDs

To study the CL behaviour of SQDs, the effect of typically utilized oxidants in CL reactions such as $KMnO_4$, $K_3Fe(CN)_6$, Ce(IV), H_2O_2, and $NaIO_4$ was investigated on the SQD solution. The experimental conditions including the oxidant concentration and amount of SQDs were optimized for each of mentioned oxidants to obtain the maximum CL intensity (Table S1). As can be seen in Figure 3, although all examined oxidants could elicit direct CL from the SQDs, the highest CL emission was observed for $KMnO_4$. Therefore, it was chosen as the best oxidant for the direct CL reaction with SQDs. To confirm this fact that the observed CL emission arose from SQDs, a control experiment with the used reagents in the synthesis of SQDs (the mixture of sulfur powder, PEG-400, and NaOH) was also performed. No significant CL signal was observed for the control reaction that confirmed the CL emission was related to the interaction between SQDs and $KMnO_4$. As shown in the kinetic profile of SQDs–$KMnO_4$ (Figure 4), this CL reaction was so fast and reached a maximum intensity within 1 s after the introduction of the oxidant solution.

3.3 | Possible mechanism of CL reaction

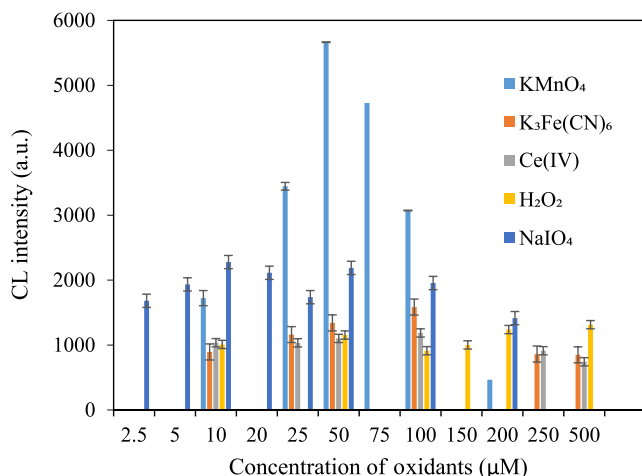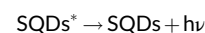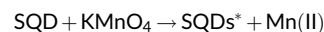We studied the CL mechanism of the SQDs–$KMnO_4$ reaction to distinguish the emitting species, and by performing the following experiments. At first, to determine the wavelength range of the CL emission various optical filters were applied. The results indicated that the CL emitted light was placed in the range 400–600 nm, which was similar to the fluorescence spectrum range of the SQDs (Figure 2b).

We also recorded the CL spectrum of the SQDs–$KMnO_4$ system using a spectrofluorimeter in flow mode. The obtained spectrum (Figure S3) indicated an emission band in the range 350–550 nm with a maximum at ~450 nm, which was similar to the SQDs fluorescence spectrum with a 360 nm excitation wavelength. Based on this fact, the CL emission can be ascribed to the excited SQDs, which are produced from the interaction between SQDs and $KMnO_4$. Furthermore, the influence of SQDs on the UV–vis absorption spectrum of $KMnO_4$ was investigated. As can be seen in Figure S4, the absorbance bands of $KMnO_4$ disappeared after adding the SQDs, in addition, the fluorescence intensity of SQDs decreased in the presence of $KMnO_4$. These facts confirmed a chemical reaction between SQDs and $KMnO_4$. According to these facts, the CL reactions can be schematically introduced as follows:

$$SQD + KMnO_4 \rightarrow SQDs^* + Mn(II)$$

$$SQDs^* \rightarrow SQDs + h\nu$$

Apparently, the CL behaviour of SQDs is the same as that of other QDs such as silicon, carbon, and graphene QDs.[42-44] The electron- and hole-injected SQDs, generated from their reaction with oxidant and produced radical oxygen species can interact together and annihilate (more discussion and passible reactions were reported in the supporting information). As a result of this phenomenon, excited SQDs can be produced, which return to the initial states with light emission.

FIGURE 3 Effect of the concentration of different oxidants on the CL intensity of SQDs. All oxidants were in basic medium (NaOH, 10 mM) except Ce(IV), which was prepared in sulfuric acid medium (0.2 M).
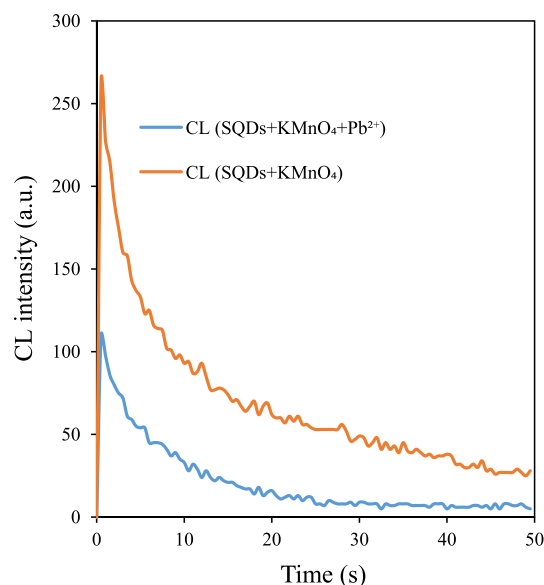

FIGURE 4 Kinetic profile of the SQDs–$KMnO_4$ CL system in the absence or presence of Pb^{2+}. Conditions: 200 μl SQDs (3 g L^{-1}); $KMnO_4$, 50 μM; and NaOH, 10 mM

3.4 | SQDs–KMnO$_4$ CL reaction for Pb ion detection

The analytical applicability of the introduced CL reaction was investigated and the effect of some metal ions was examined on the SQD–KMnO$_4$ CL system under obtained optimum experimental conditions [hydrothermal synthesis time (4 h), SQDs (0.6 g L^{-1}), KMnO$_4$ (50 μM) and NaOH (10 mM), reported in ESI; Figure S5]. As shown in Figure 4, the CL intensity of this system decreased considerably in the presence of Pb^{2+}. Conversely, the other cations indicated no significant influence on the CL intensity (Figure 5). The diminution of the CL signal can be ascribed to the interaction of Pb^{2+} with SQDs and KMnO$_4$. According to the literature, Pb^{2+} can interact with SQDs by binding to sulfur and oxygen atoms, leading to the aggregation of SQDs and quenching their emission.[17] For confirmation of the mentioned assertion, the effect of Pb^{2+} concentration on the fluorescence of SQDs was examined. As indicated in Figure S6a, the fluorescence of SQDs diminished with adding Pb^{2+}, which confirms the interaction between Pb^{2+} and SQDs. Conversely, the redox reaction can take place between Pb^{2+} and KMnO$_4$ under alkaline conditions[45] that results in consuming KMnO$_4$ in the CL system and decreasing the CL signal. The observed changes in KMnO$_4$ absorbance in the presence of Pb^{2+} confirmed the reaction between Pb^{2+} and KMnO$_4$ (Figure S6b).

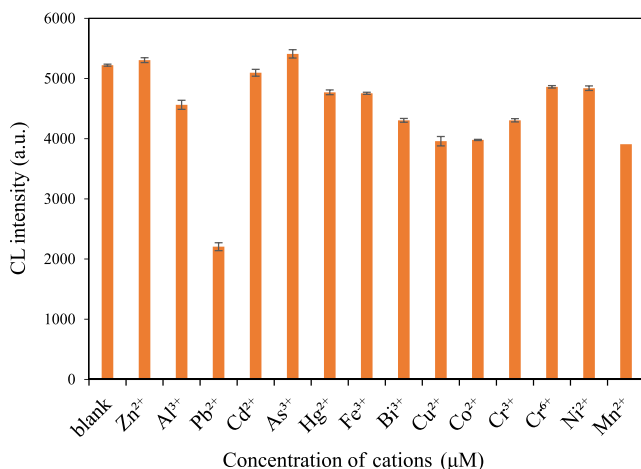Our investigation indicated that the decrease in the SQDs–KMnO$_4$ CL signal was proportional to the Pb^{2+} concentration. So, we exploited the SQDs–KMnO$_4$ CL system to design a probe for detection of Pb^{2+}. As can be seen in Figure S7 (inset), the CL emission of the SQDs–KMnO$_4$ system was linearly quenched with increasing Pb^{2+} concentration in the range 0.05–2 μM. The calibration curve is indicated in Figure S5 and the regression equation was obtained as $\Delta I = (7 \times 10^8)\, C + 507.4$ ($R^2 = 0.9916$), where $\Delta I = I_0 - I$ is the difference between the CL intensity in the absence (I_0) and presence (I) of Pb^{2+}, and C is the concentration of Pb^{2+} (μM). The detection limit was calculated as 16 nM (S/N = 3) and the relative standard deviation (RSD) was 2.6% for five repetitive measurements of Pb^{2+} (0.1 μM). The comparison of the developed method with some other reported CL methods for determination of Pb^{2+} is presented in Table 1. It is clear that the figures of merit for the developed method were better than that of some already reported methods. Although some reported methods are highly sensitive, they are complicated with multiple steps.[38,46] However, our proposed method has advantages such as simplicity and low cost.

3.5 | Study of interferences

The selectivity of the proposed method was evaluated by investigating the effect of some ions usually found in water samples on the determination of 1.0 μM Pb^{2+}. The tolerance limits for interfering species (as concentration ratios) with a relative error of <5% (for three replicate measurements) are reported in Table 2. The obtained results revealed that the method has desirable selectivity for the measurement of Pb^{2+} in water samples.

FIGURE 5 Effect of some heavy cations on the CL intensity of SQDs–KMnO$_4$

TABLE 2 Interfering species in the detection of 1 μM Pb^{2+}

Interfering species	Interfering species to analyte ratio
Na$^+$, K$^+$, Zn^{2+}, Cl$^-$, NO$_3^-$	5000
F$^-$	4000
SO$_3^{2-}$	3000
HCO$_3^-$, S$_2$O$_3^{2-}$	2500
Al^{3+}, SO$_4^{2-}$, PO$_4^{3-}$	1500
Cr^{6+}, Cd^{2+}, As^{3+}, Mg^{2+}	500
Fe^{3+}, Hg^{2+}	200
Ni^{2+}, Cr^{3+}, Bi^{3+}	100
Mn^{2+}, Co^{2+}, Cu^{2+}	5

TABLE 1 Comparison of the analytical parameters of Pb^{2+} detection in this study with similar CL studies

CL system	Linear range (μM)	LOD (nM)	Spiked concentration in water samples (μM)	References
Luminol–H$_2$O$_2$	0.007–0.125	5	0.0–0.225	[38]
Lucigenin–H$_2$O$_2$	50–440	200	50, 250, 440	[39]
Luminol–H$_2$O$_2$	0.005–1	0.79	0.015	[46]
Luminol–KMnO$_4$	0.048–48	24	–	[47]
SQDs–KMnO$_4$	0.05–2	16	0.2, 0.5, 2	This work

Sample	Spiked (μM)	Found (μM) ± SD	Recovery (%) ± RSD	t-statistic
Spring water	0	–	–	–
	0.2	0.19 ± 0.01	96.7 ± 5.6	1.0
	0.5	0.47 ± 0.01	95.2 ± 2.7	3.2
	2	2.05 ± 0.09	102.8 ± 4.8	1.0
Tap water	0	–	–	–
	0.2	0.20 ± 0.01	100.6 ± 4.3	0.2
	0.5	0.51 ± 0.03	101.4 ± 4.9	0.4
	2	1.93 ± 0.02	96.6 ± 1.4	4.2
Well water	0	–	–	–
	0.2	0.19 ± 0.01	96.0 ± 4.7	0.8
	0.5	0.49 ± 0.03	98.0 ± 3.4	0.5
	2	1.92 ± 0.03	96.1 ± 2.0	3.5

TABLE 3 Determination of Pb^{2+} in water samples

P-value = 0.05; t-critical = 4.3; n = 3.

3.6 | Analysis of real samples

To evaluate the applicability of the proposed method in real sample analysis, it was exploited to determine Pb^{2+} in spring, tap, and well water samples. The tolerance limit of Pb^{2+} in drinking water is recommended at 0.015 mg L^{-1} by the Environmental Protection Agency (EPA).[48] The Pb^{2+} concentrations around this limit were spiked into all water samples and the average recoveries were obtained of between 95.2 and 102.8%. The results are shown in Table 3. According to statistical analysis using Student's t-test, there was not any significance difference between the found and added values.

4 | CONCLUSION

In this work, SQDs were prepared from sulfur powder and PEG-400 in alkaline solution using a simple hydrothermal method. The CL behaviour of the prepared SQDs versus some oxidant such as $KMnO_4$, $K_3Fe(CN)_6$, Ce(IV), H_2O_2, and $NaIO_4$ was examined. The most CL signal of SQDs was achieved using the $KMnO_4$ and the CL mechanism of SQDs–$KMnO_4$ was studied. It was indicated that the emitting species of this reaction are SQDs* that can be produced as a result of the chemical reaction between SQDs and $KMnO_4$. Furthermore, the SQDs–$KMnO_4$ CL reaction was applied for the establishment of a novel, simple and cheap CL method for Pb^{2+} detection. The developed method was utilized for sensing Pb^{2+} in spring, tap, and well water with satisfactory results.

CONFLICTS OF INTEREST

The author(s) declare that they have no competing interests.

ORCID

Abdolhossein Naseri https://orcid.org/0000-0001-7088-5017
Tooba Hallaj https://orcid.org/0000-0001-9825-6220

REFERENCES

[1] V. G. Reshma, P. V. Mohanan, *J. Lumin.* **2019**, *205*, 287.
[2] S. Silvi, A. Credi, *Chem. Soc. Rev.* **2015**, *44*, 4275.
[3] L. Ansari, S. Hallaj, T. Hallaj, M. Amjadi, *Colloids Surf., B* **2021**, *203*, 111743.
[4] G. Gao, Y.-W. Jiang, W. Sun, F.-G. Wu, *Chin. Chem. Lett.* **2018**, *29*, 1475.
[5] Q. Li, J.-T. Wu, Y. Liu, X.-M. Qi, H.-G. Jin, C. Yang, J. Liu, G.-L. Li, Q.-G. He, *Anal. Chim. Acta* **2021**, *1170*, 338480.
[6] Y. Miao, X. Wang, J. Sun, Z. Yan, *Nanoscale Adv.* **2021**, *3*, 1532.
[7] S. Morozova, M. Alikina, A. Vinogradov, M. Pagliaro, *Front. Chem.* **2020**, *8*, 191.
[8] S. Chinnathambi, S. Chen, S. Ganesan, N. Hanagata, *Adv. Healthcare Mater.* **2014**, *3*, 10.
[9] S. Li, D. Chen, F. Zheng, H. Zhou, S. Jiang, Y. Wu, *Adv. Funct. Mater.* **2014**, *24*, 7133.
[10] Y. Duan, J. Tan, Z. Huang, Q. Deng, S. Liu, G. Wang, L. Li, L. Zhou, *Carbohydr. Polym.* **2020**, *249*, 116882.
[11] Z. Huang, J. Lei, H. Ruan, Y. Gong, G. Wang, L. Zhou, *Microchem. J.* **2021**, *164*, 106031.
[12] S. Liu, J. Wang, Y. Shi, Y. Zhai, Y. Lv, P. Zhang, Z. Wang, *Spectrochim. Acta a Mol. Biomol. Spectrosc.* **2022**, *265*, 120365.
[13] G. Qiao, L. Liu, X. Hao, J. Zheng, W. Liu, J. Gao, C. C. Zhang, Q. Wang, *Chem. Eng. J.* **2020**, *382*, 122907.
[14] Z. Wang, C. Zhang, H. Wang, Y. Xiong, X. Yang, Y. Shi, A. L. Rogach, *Angew. Chem., Int. Ed.* **2020**, *59*, 9997.
[15] A. Pal, F. Arshad, M. P. Sk, *Adv. Colloid Interface Sci.* **2020**, *285*, 102274.
[16] L. Fu, A. Wang, K. Xie, J. Zhu, F. Chen, H. Wang, H. Zhang, W. Su, Z. Wang, C. Zhou, S. Ruan, *Sens. Actuators, B* **2020**, *304*, 127390.
[17] F. Arshad, M. P. Sk, *ACS Appl. Nano Mater.* **2020**, *3*, 3044.
[18] Y. Zhang, J. Liu, X. Wu, W. Tao, Z. Li, *Anal. Chim. Acta* **2020**, *1131*, 68.
[19] Q. Tan, X. An, S. Pan, H. Liu, X. Hu, *Spectrochim. Acta a Mol. Biomol. Spectrosc.* **2021**, *247*, 119122.
[20] X. Peng, Y. Wang, Z. Luo, B. Zhang, X. Mei, X. Yang, *Microchem. J.* **2021**, *170*, 106735.
[21] Z. Huang, Y. Gao, Z. Huang, D. Chen, J. Sun, L. Zhou, *Microchem. J.* **2021**, *170*, 106656.
[22] C. Lu, Y. Wang, B. Xu, W. Zhang, Y. Xie, Y. Chen, L. Wang, X. Wang, *Food Chem.* **2022**, *366*, 130613.
[23] Y. Zhou, J. Du, Z. Wang, *Talanta* **2019**, *191*, 422.

[24] M. Amjadi, Z. Abolghasemi-Fakhri, *Sens. Actuators, B* **2018**, *257*, 629.

[25] S. N. A. Shah, X. Dou, M. Khan, K. Uchiyama, J.-M. Lin, *Talanta* **2019**, *196*, 370.

[26] J. Zhang, X. Chen, Y. Li, S. Han, Y. Du, H. Liu, *Anal. Methods* **2018**, *10*, 541.

[27] H. Song, Y. Su, L. Zhang, Y. Lv, *Luminescence* **2019**, *34*, 530.

[28] H. Chen, L. Lin, H. Li, J.-M. Lin, *Coord. Chem. Rev.* **2014**, *263*, 86.

[29] J. Yao, L. Li, P. Li, M. Yang, *Nanoscale* **2017**, *9*, 13364.

[30] L. Shen, H. Wang, S. Liu, Z. Bai, S. Zhang, X. Zhang, C. Zhang, *J. Am. Chem. Soc.* **2018**, *140*, 7878.

[31] Y.-M. Fang, J. Song, J. Li, Y.-W. Wang, H.-H. Yang, J.-J. Sun, G.-N. Chen, *Chem. Commun.* **2011**, *47*, 2369.

[32] N. Singh, A. Kumar, V. K. Gupta, B. Sharma, *Chem. Res. Toxicol.* **2018**, *31*, 1009.

[33] R. Choudhury, T. K. Misra, *Colloids Surf. A Physicochem. Eng. Asp.* **2018**, *545*, 179.

[34] M. Chen, M. Hassan, H. Li, Q. Chen, *Microchim. Acta* **2020**, *187*, 1.

[35] B. Zhang, C. Wei, *Talanta* **2018**, *182*, 125.

[36] L. Xu, X. Suo, Q. Zhang, X. Li, C. Chen, X. Zhang, *Foods* **2020**, *9*, 305.

[37] H. Wang, D. M. Wang, C. Z. Huang, *Analyst* **2015**, *140*, 5742.

[38] J. Zheng, J. L. Wai, R. J. Lake, S. Y. New, Z. He, Y. Lu, *Anal. Chem.* **2021**, *93*, 10834.

[39] P. H. Saleem, H. M. Abdullah, S. A. Yasin, *IOP Conf. Ser. Mater. Sci. Eng.* **2021**, *1058*, 12076.

[40] L. Xiao, Q. Du, Y. Huang, L. Wang, S. Cheng, Z. Wang, T. N. Wong, E. K. L. Yeow, H. Sun, *ACS Appl. Nano Mater.* **2019**, *2*, 6622.

[41] D. Chen, S. Li, F. Zheng, *Anal. Methods* **2016**, *8*, 632.

[42] Z. Ding, B. M. Quinn, S. K. Haram, L. E. Pell, B. A. Korgel, A. J. Bard, *Science* **2002**, *296*, 1293.

[43] M. Amjadi, J. L. Manzoori, T. Hallaj, M. H. Sorouraddin, *Spectrochim. Acta a Mol. Biomol. Spectrosc.* **2014**, *122*, 715.

[44] M. Amjadi, J. L. Manzoori, T. Hallaj, *J. Lumin.* **2014**, *153*, 73.

[45] X. Qi, F. Xie, *Chem. Eng. J.* **2018**, *351*, 22.

[46] Z.-M. Zhou, Y. Yu, M.-Z. Zhang, J. Chen, Q.-Q. Ren, J.-T. Song, B. Liu, Z.-Y. Ma, Y.-D. Zhao, *Sens. Actuators, B* **2014**, *201*, 496.

[47] P. Qu, S. C. Yan, H. Lu, Z. H. Lu, *Microchim. Acta* **2008**, *163*, 321.

[48] G. Aragay, J. Pons, A. Merkoçi, *Chem. Rev.* **2011**, *111*, 3433.

SUPPORTING INFORMATION

Additional supporting information can be found online in the Supporting Information section at the end of this article.